Water contrast between Precambrian and Phanerozoic continental lower crust in eastern China

Xiao-Zhi Yang, Etienne Deloule, Qun-Ke Xia, Qi-Cheng Fan, Min Feng

Water contrast between Precambrian and Phanerozoic continental lower crust in eastern China

Xiao-Zhi Yang,[1,2] Etienne Deloule,[2] Qun-Ke Xia,[1] Qi-Cheng Fan,[3] and Min Feng[1]

Received 4 December 2007; revised 19 May 2008; accepted 5 June 2008; published 19 August 2008.

[1] The presence of water, even in small amounts, in the continental lower crust may play a critical role in its physical and chemical properties and behavior. However, the environment and evolution of water in the deep crust remain poorly constrained. Investigation of water, dissolved as H-related point defects in minerals of lower crustal granulites, may provide clues to clarify this issue. The analyzed and compiled water data of nominally anhydrous clinopyroxene (cpx), orthopyroxene (opx), and plagioclase (plag) in lower crustal granulites from Hannuoba, Nushan, and Daoxian in eastern China reveal significant contrast in water contents (ppm H_2O by weight) between Precambrian and Phanerozoic samples, e.g., 200–2330 versus 275–720 ppm for cpx, 140–1875 versus 60–185 ppm for opx, 145–900 versus 65–345 ppm for plag, and 155–1120 versus 165–360 ppm for the bulk concentrations. Our data show consistently higher water contents in the Precambrian granulites, implying a more hydrous lower crust in the Precambrian than in the Phanerozoic. Such a difference may reflect variable water contents in the original melts, indicating higher water contents in the Precambrian upper mantle or a plume source for that part of the Precambrian lower crust.

Citation: Yang, X.-Z., E. Deloule, Q.-K. Xia, Q.-C. Fan, and M. Feng (2008), Water contrast between Precambrian and Phanerozoic continental lower crust in eastern China, *J. Geophys. Res.*, *113*, B08207, doi:10.1029/2007JB005541.

1. Introduction

[2] The continental lower crust, as the interface between the upper and middle continental crusts and upper mantle, is of critical importance in the tectonic evolution of the continents and in geochemical models of the bulk Earth. The lower crust consists predominately of granulites, and granulite xenoliths brought to the surface by basaltic volcanism and granulite terrains exposed to the surface by tectonic displacements provide direct insight into the composition and nature of present and/or ancient deep crust [*Rudnick*, 1992; *Rudnick and Fountain*, 1995]. Studies performed on these samples, combined with the constraints from seismic velocity data, suggest that the lower crust is dominated by mafic assemblages [e.g., *Rudnick and Fountain*, 1995].

[3] Granulites are composed mainly of nominally anhydrous minerals (NAMs): clinopyroxene (cpx), orthopyroxene (opx), and plagioclase (plag), and the lower crust is thus traditionally considered "dry." Nevertheless, *Xia et al.* [2006] showed that granulite minerals may contain a significant amount of water in the form of structural OH. Water may fundamentally influence several physical and chemical properties of the lower crust, such as the rheology, electrical conductivity, and melting behavior. Surprisingly, despite significant analytical progress in the determination of water in NAMs [e.g., *Keppler and Smyth*, 2006], the distribution and especially the evolution of water in the continental lower crust are still poorly known, and only reports of water in upper and middle crusts and in igneous feldspars and very few data on lower crustal minerals have been published [*Johnson*, 2006, and references therein]. Here, we report water content of the main constitutive phases in mafic lower crustal granulites of different forming ages from eastern China. Combining new data with those of our former study [*Xia et al.*, 2006], we discriminate water concentrations of Precambrian and Phanerozoic continental lower crust in eastern China, with the aim of understanding a possible time-dependent distribution of water in the lower crust.

2. Geological Background and Samples

[4] The North China Craton (NCC) is one of the world's oldest continental nuclei, with crustal remnants older than 3.8 Ga [*Liu et al.*, 1992]. It is bounded to the north by the late Paleozoic–early Mesozoic Central Asian Orogenic Belt and is separated in the south from the Yangtze Craton by the Qinling-Dabie and Su-Lu high- to ultrahigh-pressure metamorphic belts. The NCC is made up largely of Archean to early Paleoproterozoic basement [*Zhao et al.*, 2001]. On the basis of differences in geology and tectonic and metamorphic pressure-temperature-time history, the craton can be

[1]CAS Key Laboratory of Crust-Mantle Materials and Environments, School of Earth and Space Sciences, University of Science and Technology of China, Hefei, China.
[2]Centre de Recherches Pétrographiques et Géochimiques, Centre National de la Recherches Scientifique, Vandoeuvre-les-Nancy, France.
[3]Institute of Geology, China Earthquake Administration, Beijing, China.

0148-0227/08/2007JB005541$09.00

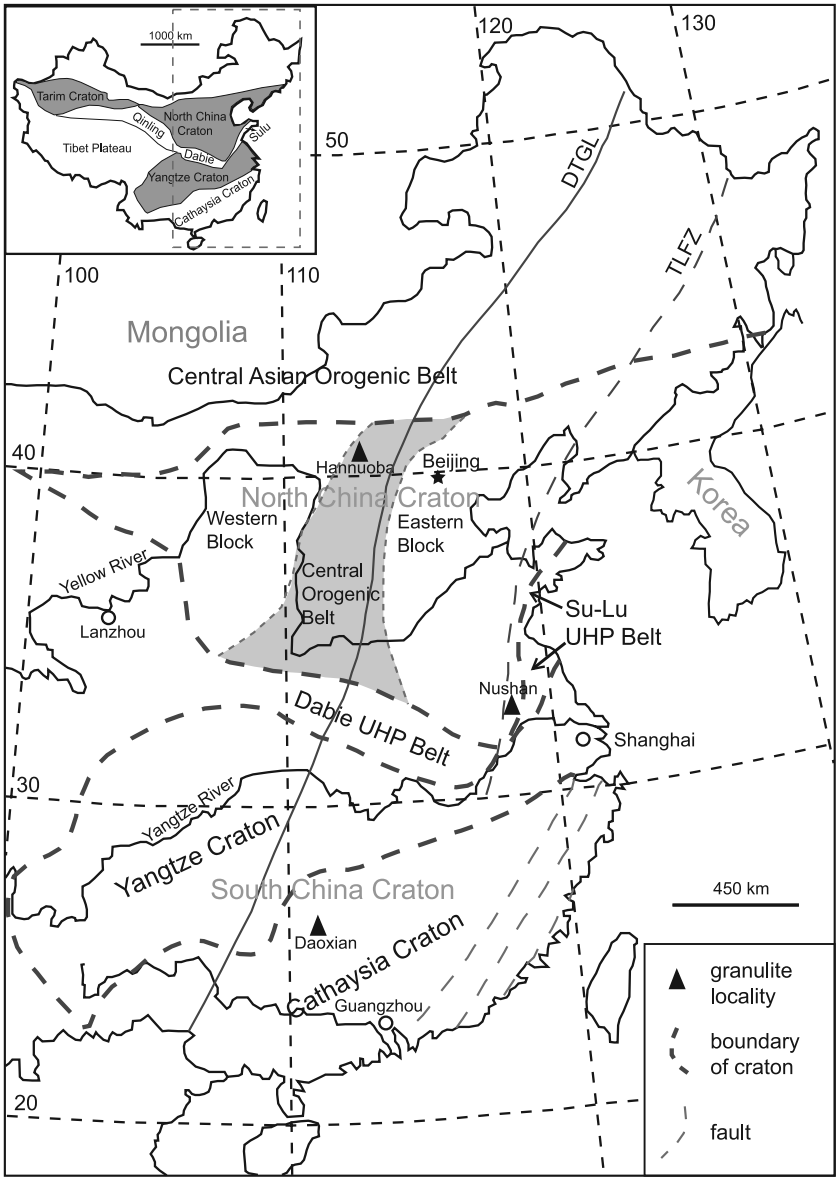

Figure 1. Locations of granulite samples in eastern China. DTGL is Daxing'anling-Taihangshan Gravity Lineament; TLFZ is Tan-Lu Fault Zone. Geological map of the Hannuoba region is given in the auxiliary material.

divided into the Eastern and Western blocks and the Central Orogenic Belt (Figure 1). The base of the Eastern and Western blocks is dominated by late Archean tonalitic, trondhjemitic, and granodioritic gneiss domes surrounded by minor supracrustal rocks, while the Central Orogenic Belt consists of late Archean amphibolites and granulites, together with some granite-greenstone terrains. The collision between the Eastern and Western blocks at ~1.8 Ga led to the formation of the Central Orogenic Belt, representing the final amalgamation of the NCC [*Zhao et al.*, 2001]. The NCC experienced widespread tectonothermal reactivation during the late Mesozoic and Cenozoic, and at least 80–140 km of the Archean lithosphere have been removed from the base [*Griffin et al.*, 1998; *Menzies et al.*, 1993].

[5] The South China Craton (SCC) is composed of the Yangtze Craton and the Cathaysia Craton (Figure 1), formed by a collage amalgamation between these two cratons during the Grenvillian-age orogeny [*Chen et al.*, 1991; *Li et al.*, 2002; *Shu and Charvet*, 1996]. The Yangtze Craton is another Archean continental nucleus in China with basement ages >3.2 Ga, as indicated by Nd and Hf model ages and sensitive high-resolution ion microprobe (SHRIMP) zircon U-Pb ages [*Gao et al.*, 1999; *Qiu et al.*, 2000; *Zhang et al.*, 2006; *Zheng et al.*, 2006]; by contrast, the Cathaysia Craton is relatively younger compared to the NCC and the Yangtze Craton. The basement of this craton is dominantly Paleoproterozoic to Mesoproterozoic, with some local late Archean component [*Chen and Jahn*, 1998]. The exposed terrains in this craton are mainly sedimentary rocks, derived from variable time periods, and magmatic rocks dominated by Mesozoic granites. The most noticeable characteristic of

geology in the Cathaysia Craton is intensive and widespread Mesozoic magmatism [*Li et al.*, 2004; *Li and Li*, 2007].

[6] Hannuoba (Figure 1) is a distinctive locality in the north edge of the NCC where both lower crustal granulite xenoliths and terrains are present. Hannuoba granulite xenoliths were captured by Cenozoic basalts and resulted dominantly from magma underplating and subsequent fractional crystallization and metamorphism between 180 and 80 Ma as indicated by zircon U-Pb dating [*Chen et al.*, 2001; *Fan et al.*, 1998; *Liu et al.*, 2001; *Wilde et al.*, 2003]. Hannuoba granulite terrains have been interpreted in terms of an exposed lower crustal section [*Zhai et al.*, 2001], which underwent two important granulite-facies metamorphic events at 2.6–2.5 and 1.9–1.8 Ga and was then uplifted to the surface at ~1.8 Ga [e.g., *Guo et al.*, 2005; *Zhai et al.*, 2005]. Preservation of kelyphite, consisting of extremely fine-grained minerals (e.g., cpx + opx + plag) around fresh garnet core in the terrain granulites [*Guo et al.*, 2005, and references therein], implies that they experienced rapid decompression and rapid cooling and thus can preserve their source information in an efficient way [*Rudnick*, 1992].

[7] Daoxian in the Hunan Province lies at the north margin of the Cathaysia Craton (Figure 1). This region, as well as the adjacent Ningyuan area, is unique in the west Cathaysia Craton for the presence of abundant lower crust and mantle xenoliths. Daoxian granulite xenoliths were entrained by Mesozoic basalts, with their ages ranging from 150 to 130 Ma, determined by K-Ar and Ar-Ar methods [*Guo et al.*, 1996; *Li et al.*, 2004; *Zhao et al.*, 1998]. They were formed through accumulation of pyroxene and plagioclase from underplating mafic melts, followed by subsequent lower crustal metamorphism in multiple episodic periods. The Sm-Nd mineral isochron age is ~220 Ma [*Guo et al.*, 1996]; the SHRIMP U-Pb dating demonstrates that most zircons from Daxian granulites have relatively young ages (200–280 Ma), although rare old (up to 850 Ma) zircons do exist [*Dai et al.*, 2008]. Therefore, the Daoxian granulites are believed to have formed in the Mesozoic in accordance with extensive Mesozoic magmatism in this area [*Li et al.*, 2004; *Li and Li*, 2007].

[8] The samples analyzed for this study include 8 xenolith and 10 terrain granulites from Hannuoba and 14 xenolith granulites from Daoxian (Table 1). They are characterized, in thin sections, by medium- to fine-grained granoblastic fabrics or heteroblastic and/or near-equigranular textures. Hypersthene is very common in all these samples; mineralogical banding composed of plag-rich and pyroxene-rich layers can be found in almost all of these samples. All these samples are two-pyroxene granulites, and their compositions range from dominantly mafic to less intermediate [*Dai et al.*, 2008; *Liu et al.*, 2001]. These suggest that they originate from igneous mafic cumulates subject to the lower crustal metamorphism, as proposed by *Guo et al.* [2005], *Liu et al.* [2001], and *Dai et al.* [2008]. These samples are all well preserved with no hydrous phases or observable alteration, except for some Hannuoba terrain granulites in which amphibole is found in minor amounts (<3%) (Table 1) and for Daoxian xenolith granulites in which alteration of opx into chloride is often observed, but cpx are always very fresh [see also *Dai et al.*, 2008]. According to the age patterns, these samples are simply divided into Precambrian (Hannuoba terrain granulites) and Phanerozoic (Hannuoba and Daoxian xenolith granulites) groups (Table 1).

[9] To obtain a more general comparison of water content, the water data on the Nushan xenolith granulites reported by *Xia et al.* [2006] were also compiled here. The Nushan xenolith granulites were entrained by Cenozoic basalts, but zircon U-Pb dating indicates mostly two episodes of ~2.5 Ga and ~1.9 Ga for their formation. This, coupled with trace element modeling, Sr-Nd isotope systematics, and similarities in seismic velocity and major element compositions, led *Huang et al.* [2004] to suggest that Nushan granulites were mainly derived from the late Archean crystalline basement with very weak, if any, effects from subsequent mafic underplating and only subordinately derived from the mafic layer newly accreted during the late Mesozoic and that they can be used as a proxy for early lower crust. These samples were allotted to the Precambrian group in this paper.

3. Analytical Methods

[10] Mineral compositions were determined by CAMECA SX50 and SX100 electron microprobes at the University Henri Poincaré in Nancy for the Hannuoba xenolith and terrain granulites and by a JEOL JXA-8100 superprobe at Nanjing University, China, for the Daoxian xenolith granulites, following similar conditions: 10 nA beam current, 15 kV accelerated voltage, and natural and synthetic standards, calibrated by *Pouchou and Pichoir* [1985] and atomic number, absorption, and fluorescence corrections, respectively. Two to three points (from core to rim) for each grain and three to five grains for each mineral in the same sample were analyzed. Densities of the minerals in the studied granulites were estimated from the proportion and the density of end-member minerals [*Deer et al.*, 1992]: Wo 2.98 g cm^{-3}, En 3.21 g cm^{-3}, Fs 3.96 g cm^{-3}, An 2.76 g cm^{-3}, Ab 2.55 g cm^{-3}, and Or 2.63 g cm^{-3}. The variation of the calculated density for a mineral is <3% between different samples from the same locality and <6% between different localities. For each suite of granulites, the average density of individual minerals was used in the calculation of the bulk water content.

[11] Fourier transform infrared (FTIR) measurements were conducted following *Katayama et al.* [2006] and *Xia et al.* [2006]. Infrared spectra were obtained at wave numbers from 650 to 6000 cm^{-1} using a Nicolet 5700 FTIR spectrometer coupled with a Continuμm microscope at the University of Science and Technology of China. The samples were measured by unpolarized radiation with an IR light source, a KBr beam-splitter, and a liquid nitrogen–cooled mercury-cadmium-tellurium narrowband, high-sensitivity detector. For each spectrum, 128 or 256 scans were accumulated at a 4 cm^{-1} resolution. Optically clean, inclusion- and crack-free areas, usually centered in the core region of each grain, were selected for the measurements with apertures of 30 × 30 or 50 × 50 μm. A golden wire-grid polarizer was applied on some oriented crystals, and some large and fresh grains were selected for the H profile analysis. Accurate quantitative measurement of hydrogen species in anisotropic minerals requires the preparation of oriented single crystals and the use of polarized IR radiation [*Libowitzky and Rossman*, 1996]. However, performing

Table 1. Summary of Petrographic Features for Granulites From Eastern China[a]

Samples	Model Mineralogy	Description
	Precambrian	
Hannuoba terrain		
MJ9801	cpx30opx12plag30grt23mt2amp3	fine grain, near-equigranular texture
MJ9803	cpx30opx13plag55mt2	banded, fine grain
MJ9805	cpx30opx10plag40grt15mt5	banded, fine grain
MJ9806	cpx30opx7plag55mt5amp3	less banded, fine grain
MJ9807	cpx35opx10plag50mt5	banded, fine grain
MJ9808	cpx40opx7plag50mt3amp2	fine grain, near-equigranular texture
MJ9810	cpx45opx20plag25grt5mt3amp2	banded, fine grain
MJ9811	cpx35opx12plag45grt5mt3	fine grain, near-equigranular texture
SX-1	cpx25opx5plag50grt15mt3amp2	banded, fine grain (large grt grains)
SX-2	cpx28opx5plag40grt23mt3amp1	banded, fine grain
	Phanerozoic	
Hannuoba xenolith		
WD9520	cpx45opx20plag35	banded, medium to coarse grain, near-equigranular texture
WD9522	cpx30opx50plag20	banded, medium grain, heteroblastic texture
WD9530	cpx45opx25plag30	banded, medium to coarse grain, near-equigranular texture
WD9532	cpx55opx25plag20	banded, medium grain, granoblastic, near-equigranular texture
WD9546	cpx55opx35plag10	less banded, medium grain, granoblastic, heteroblastic texture
DM9855	cpx30opx25plag45	banded, medium to coarse grain, near-equigranular texture
DM9871	cpx25opx10plag65	banded, medium grain, granoblastic, near-equigranular texture
HD71	cpx50opx35plag15	banded, medium grain, near-equigranular texture
Daoxian xenolith		
DX01	cpx40opx30plag30	medium to fine grain, near-equigranular texture
DX03	cpx35opx10plag54sp1	banded, medium to coarse grain
DX04	cpx20opx20plag60	banded, medium to fine grain
DX06	cpx30opx20plag49sp1	banded, medium to fine grain
DX10	cpx30opx25plag44sp1	banded, medium to fine grain
DX12	cpx25opx10plag64sp1	banded, medium to fine grain
DX13	cpx40opx19plag40sp1	banded, medium to coarse grain
DX19	cpx20opx15plag54sp1	banded, medium to coarse grain
DX20	cpx30opx15plag54sp1	banded, medium to fine grain
DX28	cpx35opx20plag45	less banded, fine grain
DX31	cpx65opx20plag14sp1	medium to fine grain, heteroblastic texture
DX34	cpx20opx10plag70	less banded, fine grain
DX40	cpx30opx10plag59sp1	less banded, coarse grain
DX44	cpx35opx20plag44sp1	banded, medium to coarse grain

[a]Abbreviations are grt, garnet; amp, amphibole; sp, spinel; and mt, magnetite. Samples labeled MJ and SX in the Hannuoba terrain granulites are from Manjinggou and Xiwangshan at the Hannuoba region, respectively; Hannuoba granulite xenoliths are from Damaping at the Hannuoba region (see auxiliary material for the illustration of these localities).

such a treatment on fine-grained natural granulites is extremely difficult. And so here, where unpolarized determinations were made, we instead analyzed a significant number of individual grains (e.g., 8–25) of each mineral in the same sample, whose orientations are highly variable as revealed by our FTIR results (see section 4), and their average value was used to determine the water content, as were the values of *Grant et al.* [2007], *Katayama and Nakashima* [2003], *Katayama et al.* [2006], and *Xia et al.* [2005, 2006]. The possible effects from nonstructural OH/H_2O on some spectra (e.g., of garnet) were resolved by using the Peakfit V4.12 program (Jandel Scientific) based on a Gaussian function.

[12] Water contents were calculated by the modified form of the Beer-Lambert law:

$$\Delta = I \times c \times t \times \gamma,$$

where Δ is the integral absorption area (cm^{-1}) of absorption bands, I is the integral-specific absorption coefficient (ppm^{-1} cm^{-2}), c is the content of hydrogen species (ppm H_2O weight), t is the thickness of the section (cm), and γ is the orientation factor discussed by *Paterson* [1982]. In this paper, the integral region was $2700 \sim 3800$ cm^{-1} with the integral-specific coefficient of 7.09 ppm^{-1} cm^{-2} for cpx, 14.84 ppm^{-1} cm^{-2} for opx, and 1.36 ppm^{-1} cm^{-2} for garnet from *Bell et al.* [1995] and 15.3 $ppm^{-1}{\cdot}cm^{-2}$ for plagioclase from *Johnson and Rossman* [2003]. Thickness was measured with a digital micrometer and reported as an average of $30 \sim 40$ measurements covering the whole section; the orientation factor of 1/3 was applied in the calculation for anisotropic cpx, opx, and plag, and a factor of 1 was applied for isotropic garnet [*Paterson*, 1982]. Baseline corrections were carried out with a spline fit method by points outside the OH-stretching region.

[13] Possible factors influencing the calculated results include the following.

[14] 1. Unpolarized light is the main uncertainty during the analysis, but it is estimated to be mostly less than 10% considering the treatment (averaging 8–25 individual grains with variable absorbance) [*Asimow et al.*, 2006; *Sambridge et al.*, 2008; *Kovács et al.*, 2008].

[15] 2. Another possible factor is baseline correction. The background could be treated as a flat curve along the trend of our spectra in most cases, and the difference between different baseline corrections, e.g., spline fit or polynomial

fit or slightly changing the points during the fitting, is usually <5%.

[16] 3. A third possible factor is the variation of sample thickness on the thin sections. On each section, 30–40 thickness measurements point out that variations are less than 6% in our samples.

[17] 4. Extinction coefficients may influence results. There are slight differences between cpx, opx, and garnet in our granulite samples and those used to determine the mineral-specific absorption coefficients [*Bell et al.*, 1995], but the variation is generally <8% in their compositions and densities, and it is even less than 2% for plag relative to those used by *Johnson and Rossman* [2003]. The error caused by the coefficients is therefore estimated to be <10%. The total uncertainty is estimated to be less than 30%.

4. Results

[18] Electron microprobe measurements show that the individual minerals are homogeneous for each sample (the averaged data are provided in the auxiliary material).[1] These results are very similar to those reported by *Chen et al.* [2001] and *Liu et al.* [2001] for the Hannuoba mafic xenolith granulites, by *Fan et al.* [2005] for the Hannuoba terrain granulites, and by *Dai et al.* [2008] for the Daoxian xenolith granulites.

[19] Following the protocol suggested by *Xu et al.* [1998], equilibrated pressure-temperature (P-T) conditions were calculated by the geobarometer of *Wood* [1974] for garnet-bearing samples and the two-pyroxene geothermometers of *Wood and Banno* [1973] and *Wells* [1977]. Pressures of xenoliths were estimated by using the geotherm established by *Chen et al.* [2001] in the Hannuoba region and by the P-T estimation of *Dai et al.* [2008] in the Daoxian region. The temperatures obtained by the two-pyroxene geothermometers of *Wood and Banno* [1973] and of *Wells* [1977] agree to within ±50°C for most samples, which is consistent with the calculation uncertainties. The estimated results are 780–860°C and 1.0–1.5 GPa for the Hannuoba terrain granulites, 860–920°C and 0.9–1.2 GPa for the Hannuoba granulite xenoliths, and 850–900°C and 0.9–1.2 GPa for the Daoxian granulites, so they are in good agreement with previous reports [*Chen et al.*, 2001; *Dai et al.*, 2008; *Guo et al.*, 2005; *Liu et al.*, 2001; *Zhai et al.*, 2005]. These P-T data indicate that the granulites were at equilibrium in the lower and lowermost crust beneath the Hannuoba and Daoxian regions (the estimated crust-mantle boundary is ~42 km at Hannuoba [*Chen et al.*, 2001] and ~40 to 45 km at Daoxian [*Dai et al.*, 2008]); the same conclusion was reached by *Xia et al.* [2006] for Nushan xenolith granulites.

[20] FTIR spectra (Figure 2) show that all the spectra of cpx, opx, plag, and garnet have several absorption bands in the range of 3000 to 3750 cm^{-1}, which can be divided into several different groups for each mineral. The different bands are common in all the samples, with the exception of high-absorption bands only found in some terrain granulites. The position and shape of these bands are similar to those reported for individual minerals [*Bell et al.*, 1995; *Bell and Rossman*, 1992; *Johnson and Rossman*, 2004; *Skogby et al.*, 1990; *Skogby and Rossman*, 1989; *Stalder and Skogby*, 2002]. Slight differences may be associated with the chemical composition and crystal structure of the hosted phases. The relative absorbances of bands for anisotropic cpx, opx, or plag are variable for different grains even in the same sample, which are attributed to variable orientations of the grains with respect to the infrared beam direction and to possible water heterogeneity. Polarized analyses performed on some oriented grains show a significant dependence of the OH absorbance on the polarized orientation for these different bands (Figure 3), attesting that they result from the vibration of structural OH. Molecular H_2O may also occur in our plag based on the characteristic bands at ~3620, ~3550, and ~3440 cm^{-1} as reported by *Johnson and Rossman* [2004]. The 3420–3450 cm^{-1} band of garnet is out of the energy range of structural OH, usually 3500–3700 cm^{-1}, in previous studies on both natural and synthesized garnets, and is commonly ascribed to tiny fluid inclusions [*Langer et al.*, 1993; *Rossman and Aines*, 1991; *Rossman et al.*, 1989], and they are therefore removed from the calculation of water content by the Peakfit treatment; some spectra also display weak absorbance in the range of 3700–3800 cm^{-1}, which is probably an artifact due to the light source in the Nicolet instrument (G. Rossman, personal communication, 2004), and were also excluded from the calculation of water content.

[21] H profile analyses performed on selected pyroxene grains in each suite of granulites reveal very weak variations of OH absorbance from core to rim regions, ranging mostly from 5 to 10% and in rare cases a little higher up to ~20% (see auxiliary material). No apparent variations beyond the analytical uncertainty (30%) were found for H absorbances in large pyroxene grains in the granulites, implying the absence of significant exchange/diffusion loss of H between melts and minerals during their exhumation. The calculated average H_2O contents, as well as the compiled Nushan data from *Xia et al.* [2006], are presented in Table 2, and the OH content of garnet for individual grains in the Hannuoba terrain granulites is given in Table 3.

[22] The water contents are highly variable. They range on average from 275 to 720 ppm for cpx, 60 to 185 ppm for opx, 65 to 205 ppm for plag, and 165 to 355 ppm for bulk rock in the Hannuoba xenolith granulites; from 585 to 1480 ppm for cpx, 230 to 1875 ppm for opx, 175 to 895 ppm for plag, 290 to 620 ppm for garnet, and 405 to 1120 ppm for bulk rock in the Hannuoba terrain granulites; and from 285 to 500 ppm for cpx, 65 to 135 ppm for opx, 205 to 345 ppm for plag, and 200 to 360 ppm for bulk rock in the Daoxian xenolith granulites. These variations are roughly similar to those observed in the Nushan xenolith granulites [*Xia et al.*, 2006] (see also cited data in Table 2). OH content of garnet in the terrain samples demonstrates large variations, ranging from 0, with grains without any evident H-related IR absorption (Figure 2), to more than 1000 ppm (Table 3); similar variations were reported for garnet from the central Dabieshan eclogites by *Xia et al.* [2005] and for garnet from the skarn belt in Oak Hill and Willsboro, Adirondacks, by *Johnson* [2006]. The above mentioned variations of water content for either individual minerals, bulk contents, or different garnet grains are far beyond the estimated uncer-

[1] Auxiliary materials are available in the HTML. doi:10.1029/2007JB005541.

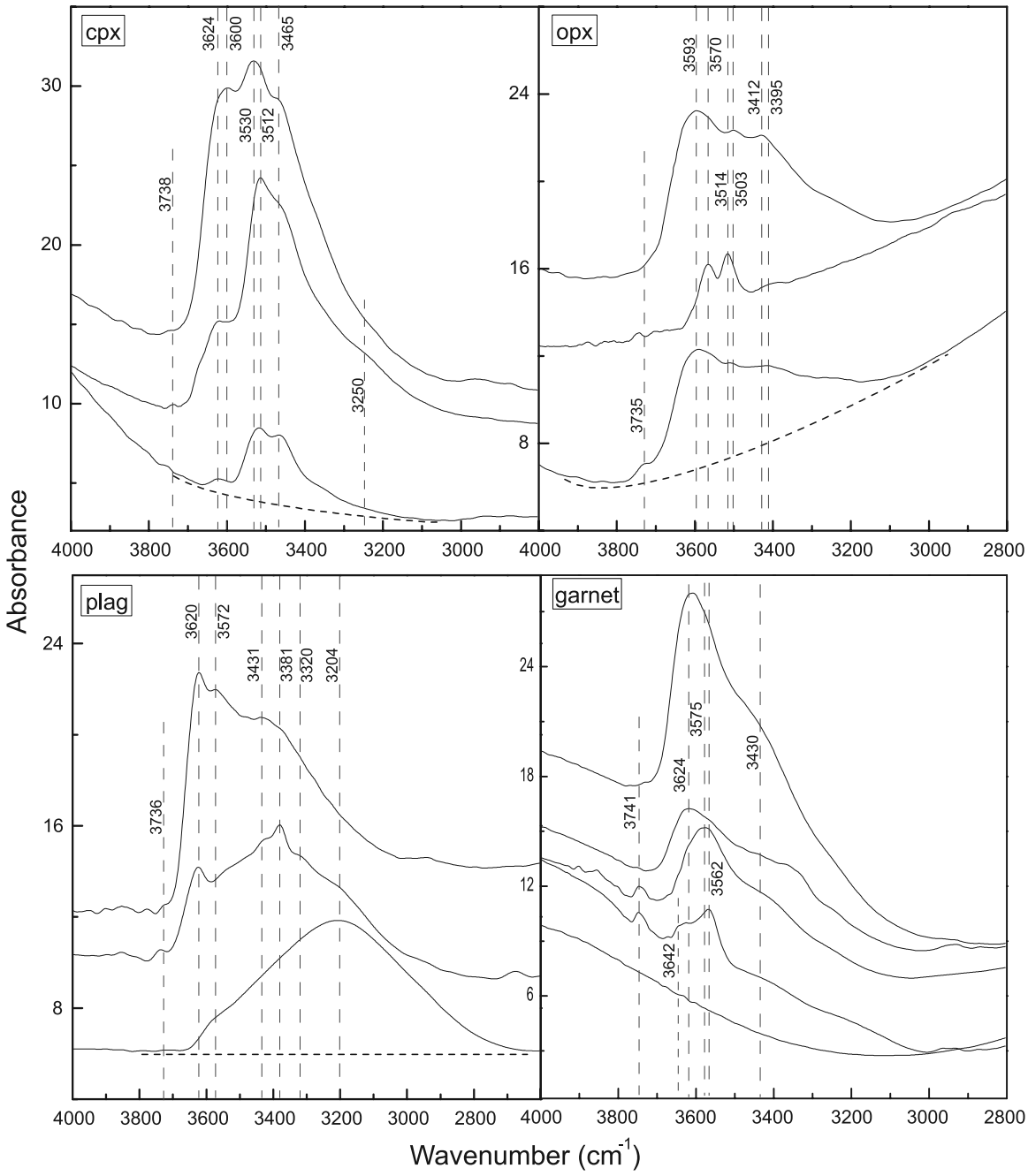

Figure 2. Representative Fourier transform infrared (FTIR) spectra of cpx, opx, plag, and garnet in the granulites. Dashed lines show where the baseline was taken by spine fit method; spectra were normalized to 1 cm thickness and offset for clarity.

tainty (30%), indicating heterogeneous distribution of water in the lower crust.

[23] Water contents of individual minerals and bulk rocks in the Hannuoba terrain granulites resemble those in the Nushan xenolith granulites [*Xia et al.*, 2006] (Table 2), consistent with similarities in their major/trace element compositions, formation ages, and other behaviors [*Huang et al.*, 2004], and they are remarkably higher than those in the Hannuoba and Daoxian xenolith granulites except for a few Nushan samples which have relatively lower water content (Figure 4) despite the large heterogeneities of water in these suites of granulites. Considering the age information of these samples, the Precambrian granulites appear to have higher water contents than the Phanerozoic ones (Figure 4).

5. Preservation of Initial Water Content in the Lower Crust

[24] Whether deep-seated minerals brought to the surface can preserve their original water contents is an unresolved question. It is argued that some minerals can keep their initial OH contents [e.g., *Bell et al.*, 2004; *Grant et al.*, 2007; *Peslier et al.*, 2002], but there are also studies

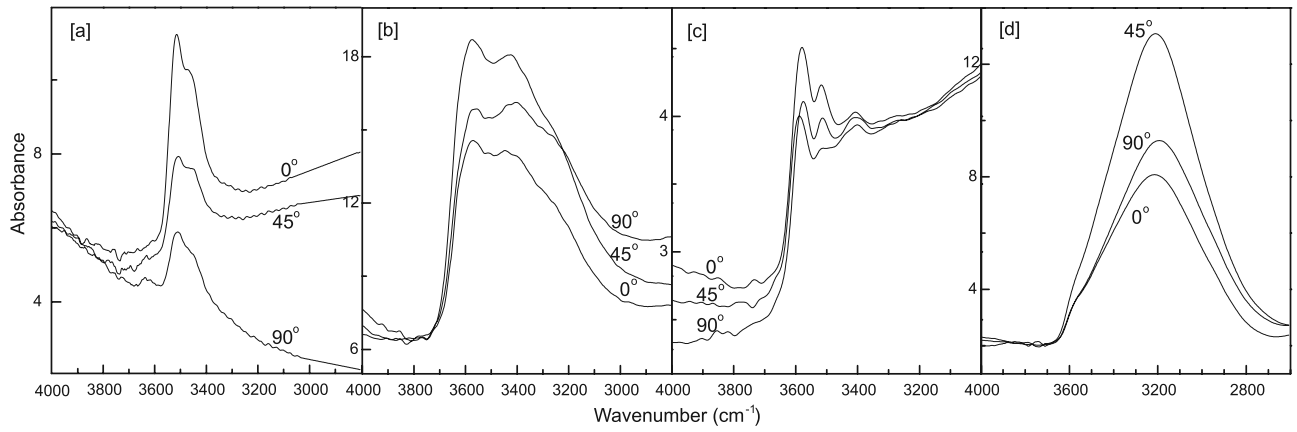

Figure 3. Representative polarized FTIR spectra of cpx, opx, and plag with polarization orientation: (a) cpx spectra from DM9855, (b) opx spectra of high water content from MJ9806, (c) opx spectra of low water content from DM9855, and (d) plag spectra from DM9855.

showing that the water content of minerals may be modified during eruption, especially by hydrogen diffusion and by exchange between crystals and fluids [e.g., *Ingrin and Skogby*, 2000].

[25] In our study, the measured H_2O data are interpreted in terms of original contents on the basis of the following characteristics.

[26] 1. Each of the phases in the same sample is chemically identical. No major element compositional zoning has been observed for the studied grains in these samples, and no rare Earth element (REE) compositional zoning has been observed in individual grains within selected Hannuoba xenolith and terrain and Nushan xenolith granulites revealed by in situ ion microprobe measurements [*Yang et al.*, 2007].

[27] 2. The FTIR measurements were usually conducted in the core region of clean, crack- and inclusion-free grains of relatively large size. It is therefore inferred that the loss of H in these areas by diffusion during the exhumation would be very weak [*Peslier and Luhr*, 2006].

[28] 3. Profile analyses on many pyroxene grains in all the granulites show that the H-related IR absorption is mostly homogeneous between their core and rim regions [*Xia et al.*, 2006; this study], indicating negligible variation of H content, possibly because of diffusional exchange.

[29] 4. The studied samples are usually very fresh, and the spectra used in the water calculation show no signal of any evident hydrous phases, which would produce sharp bonds in the region of >3660 cm^{-1}. In this case, there is no evident interference from other H-bearing phases or any exchange of H between them.

[30] 5. The hydrogen isotopic measurements by ion microprobe for both profile analyses across mineral grains and the average compositions of individual minerals in the selected Hannuoba xenolith and terrain and Nushan xenolith granulites also favor the preservation of their initial hydrogen information [*Yang et al.*, 2007].

6. Partitioning of Water Between Lower Crustal Phases

[31] The partitioning of water between lower crustal granulite mineral pairs, e.g., cpx-opx, plag-cpx, and plag-opx are shown in Figures 5a–5c. Roughly, these mineral pairs display positive relationships, although some samples deviate obviously from the trends (e.g., cpx-opx in Figure 5a). The partition coefficient of water between cpx and opx varies in the range of 0.5 to 10.2, with an average of 3.2; the coefficients are variable between different geological localities, e.g., ~6 for the Hannuoba xenolith granulites, ~1 for the Hannuoba terrain granulites, ~2.5 for the Nushan xenolith granulites, and ~4 for the Daoxian xenolith granulites (Table 2). Similar variations can also be observed for the plag-cpx and plag-opx pairs (Figures 5b and 5c). These may reflect the dependence on geological environments as argued by *Skogby et al.* [1990].

[32] Although the lack of data on water partitioning between plagioclase and pyroxenes makes it hard for a quantitative comparison with our data, available studies on natural and synthesized mantle samples have documented that the equilibrium partition coefficient of water between cpx and opx, $D^{water}_{cpx/opx}$, is about 1.9–2.3 [e.g., *Aubaud et al.*, 2004; *Bell and Rossman*, 1992; *Bell et al.*, 2004; *Grant et al.*, 2007; *Hauri et al.*, 2006; *Koga et al.*, 2003; *Peslier et al.*, 2002]. The values measured in our samples (in particular, Nushan and Daoxian granulites) (Figure 5) are similar to those mentioned above. Deviation from the equilibrium trend may be ascribed to water loss from individual grains/minerals during granulite-facies metamorphism (e.g., via mineral degassing after crystallization or water loss from the original mantle melts [*Yang et al.*, 2007]). These processes could certainly modify the initial water content of minerals inherited from their original melts or even the water content in the melts and therefore produce the observed disequilibrium. However, there are also several other scenarios which can result in such disequilibrium: (1) the equilibrium could not be acquired under the lower crustal P-T conditions, (2) the water content of lower crustal minerals was not inherited from the mantle source where they originated, or (3) closed-system redistribution of H between coexisting minerals altered their partitioning as a function of the different mineralogical composition (e.g., plagioclase-rich versus pyroxene-rich samples).

[33] The possibility exists that the equilibrium partition coefficient between mantle-derived pyroxenes should not be used for crustal rocks because of the difference in chemical composition and crystal structure (e.g., rich in

Table 2. Water Content of Main Constitutive Minerals in the Granulites From Eastern China[a]

Sample	Thickness (cm)	cpx	opx	plag	grt	Bulk
Precambrian						
Hannuoba terrain						
MJ9801	0.016	1480	1875	895	560	1120
MJ9803	0.021	665	310	265	-	405
MJ9805	0.011	1250	1480	580	-	795
MJ9806	0.017	820	1325	795	-	855
MJ9807	0.024	780	306	274	-	480
MJ9808	0.016	585	620	325	-	470
MJ9810	0.022	1175	885	345	430	875
MJ9811	0.019	1100	365	245	620	615
SX-1	0.020	1365	1285	445	291	725
SX-2	0.019	885	230	175	430	465
Nushan xenolith						
04NS1	0.025	-	290	460		435
04NS5	0.033	2330	665	725		970
04NS8	0.032	2030	590	710		790
04NS9	0.024	215	445	365		325
04NS11	0.029	-	465	450		455
04NS12	0.021	200	160	145		155
04NS13	0.026	-	140	290		260
04NS14	0.038	-	1270	900		950
04NS15	0.023	1245	550	565		645
04NS16	0.021	2330	525	820		870
Phanerozoic						
Hannuoba xenolith						
WD9520	0.019	440	65	180		275
WD9522	0.019	600	185	135		300
WD9530	0.011	470	140	205		310
WD9532	0.021	480	70	85		300
WD9546	0.015	570	90	140		355
DM9855	0.014	275	135	100		165
DM9871	0.023	720	70	90		260
HD71	0.026	470	60	65		265
Daoxian xenolith						
DX01	0.023	445	110	350		310
DX03	0.017	285	70	205		220
DX04	0.020	335	65	205		200
DX06	0.016	390	90	295		280
DX10	0.016	345	90	345		270
DX12	0.022	435	120	265		295
DX13	0.022	310	110	290		260
DX19	0.016	430	140	305		315
DX20	0.023	425	85	250		280
DX28	0.018	435	135	260		295
DX31	0.023	285	80	225		235
DX34	0.015	350	85	275		270
DX40	0.013	500	70	340		360
DX44	0.015	370	135	330		300

[a]Water contents were rounded to the nearest 5 ppm (H_2O by weight). Nushan data are referred to *Xia et al.* [2006] and are calculated by the same method used in this paper for comparison. Dash indicates not present. The thickness is an average of 30 $\sim$ 40 measurements covering the whole section (see text).

Fe in granulites versus Mg in peridotites), which may greatly influence the incorporation of H [e.g., *Skogby and Rossman*, 1989; *Stalder*, 2004]. In principle, a greater range of substitutions of trivalent and tetravalent ions, even of large size such as OH, may be accommodated by the structure of Fe-rich granulite-borne pyroxenes than by the Mg-rich pyroxene from mantle xenoliths. In fact, the mechanisms of H incorporation into minerals may be different between lower crustal and mantle P-T conditions, as recently proposed on the basis of experiments on Al-rich orthopyroxene [*Mierdel et al.*, 2007]. Further investigations are necessary for a better knowledge of the partitioning of water between lower crustal assemblages.

7. Implications for the Water Content in the Lower Crust

[34] Precambrian granulites, on average, contain more water than the Phanerozoic granulites by a factor of 2–3 or even higher (Figure 4). If they actually preserved their initial water content, as discussed in section 6, it follows that the continental lower crust of eastern China was more hydrous in the Precambrian than in the Phanerozoic era. The higher water contents in the Precambrian lower crust may have profound influences on many physical properties of lower crustal materials, such as lowering the rheological strength and melting temperatures at depth and/or modifying the seismic velocity, even on the mechanisms of crustal growth.

[35] The strong contrast in water content between the Precambrian and Phanerozoic lower crust of eastern China can be explained in the following terms.

[36] 1. While the possibility of pressure, or difference in equilibration depth, affecting the solubility of OH in minerals may to some extent influence the water content, it cannot make a large contribution to the contrast observed in the studied rocks. Granulites equilibrated at about 0.7 to 1.5 GPa, and within this pressure range, possible variations of OH content caused by pressure (e.g., <15% for cpx and <30% for opx [*Rauch and Keppler*, 2002; *Bromiley et al.*, 2004; *Mierdel et al.*, 2007]) are far smaller than those observed in the samples (Table 2 and Figure 4).

[37] 2. There is no evidence that Precambrian reequilibrated granulites with mantle melts and increased OH contents were affected by mantle melts [*Huang et al.*, 2004; *Zhai et al.*, 2005]. Furthermore, the ability for melt to percolate within a rock matrix is controlled by the dihedral angle (θ) between solid and melt, and for $\theta > 60°$, small melt fractions cannot percolate [*Waff and Bulau*, 1979]; θ between lower crustal assemblages and melt is usually larger than 60° (e.g., θ is 98° between cpx and melt) and is 76° between opx and melt [*Toramaru and Fujii*, 1986]. Thus, melt percolation through the lower crust is unlikely as is rehydration of the lower crust by mantle melts.

Table 3. Water Content of Garnet in the Hannuoba Terrain Granulites

	Analysis									
	1	2	3	4	5	6	7	8	9	10
MJ9801	982	1114	949	787	287	354	882	1337	933	618
	140	89	143	237	362	105	439	281		
MJ9810	635	569	953	558	1477	955	1132	1253		
MJ9811	490	1243	229	794	761	523	285			
SX-1[a]	62	167	124	142	191	24	140	206	60	157
	54	147	95	68	142	90	156	175	63	173
	297	322	365	358	209	581	165	79	133	408
	174	556	211	349	151					
SX-2	481	199	336	406	654	584	273	552	404	392

[a]Nearly 40 grains in sample SX-1 were analyzed because garnet is especially abundant and fresh in it; some grains in these samples actually contain no water (see text), which were not illustrated here.

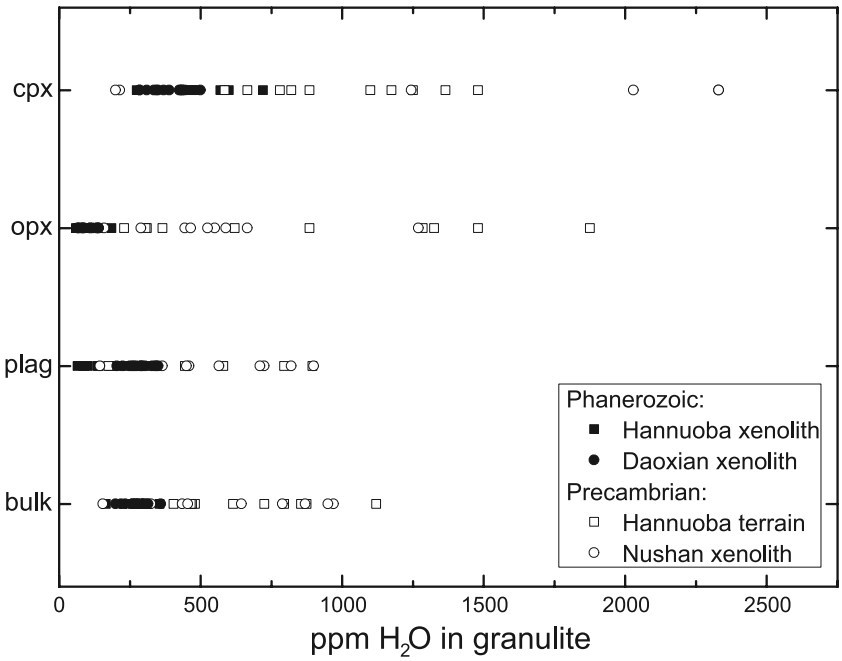

Figure 4. Water content of cpx, opx, plag, and bulk values in the granulites from eastern China.

[38] 3. During dehydration of the Phanerozoic granulites via heating and partial melting from an underplated mantle, fractional crystallization prior to and/or partial melting after the formation of these granulites might have lowered the OH contents of crustal rocks. It is suggested that the incompatible behavior of H_2O during melting and crystallization may be comparable to that of cerium [e.g., *Michael*, 1995, and references therein] and that large-ion lithophile element (LILE) and light REE (LREE) patterns could be used to infer H_2O loss besides tracing melting process. However, if the initial water contents in Precambrian and Phanerozoic granulites (or their original melts) were similar, relatively high degrees of dehydration are required to produce the measured compositions. The extent of fractional crystallization for the Hannuoba xenolith granulites has been inferred to be low to medium (5–40% [*Liu et al.*, 2001]) and consistency in REE patterns in individual minerals between the Hannuoba xenolith, Nushan xenolith,

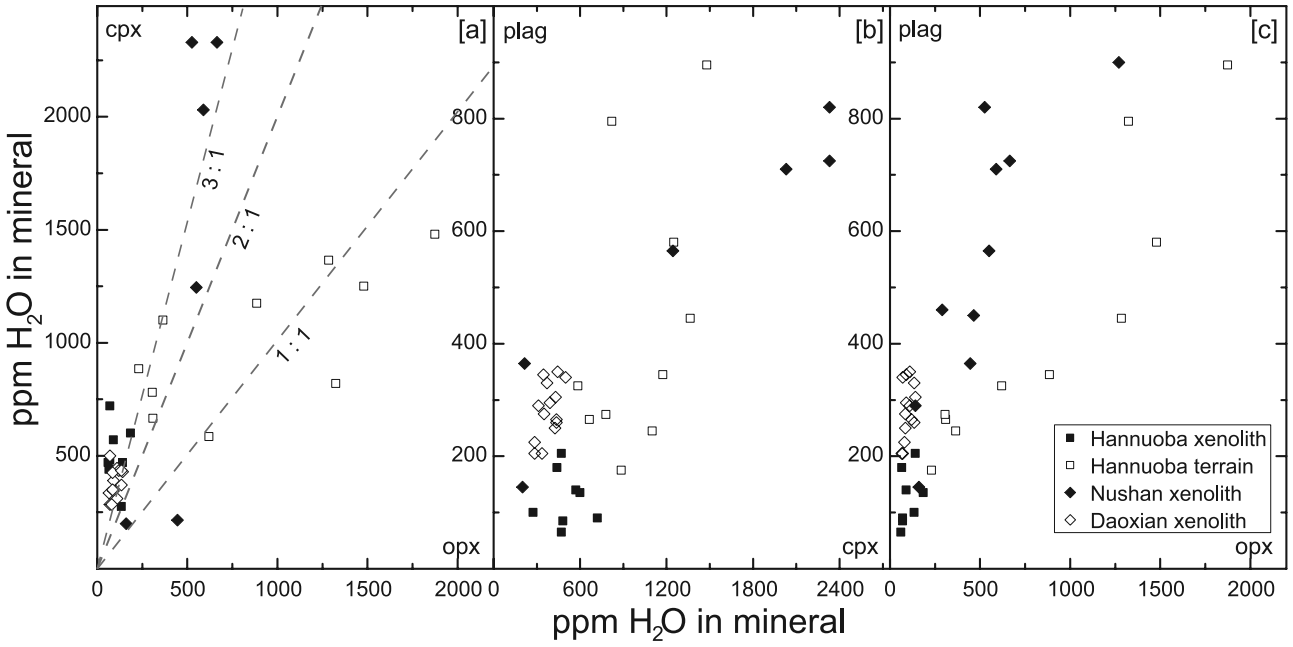

Figure 5. Partitioning of water between lower crustal granulite minerals of eastern China. Three dashed gray lines in terms of 1:1, 2:1, and 3:1 partitioning of water between lower crustal granulite mineral pairs (a) cpx-opx, (b) plag-cpx, and (c) plag-opx were drawn for reference.

and Hannuoba terrain granulites [*Yang et al.*, 2007]; undepleted LREE and LILE concentrations in bulk rocks of Hannuoba [*Liu et al.*, 2001] and Daoxian xenolith granulites [*Dai et al.*, 2008]; and the absence of simple correlations between Mg # values (index of partial melting) and Ce contents for pyroxenes in the Hannuoba xenoliths (see auxiliary material) and for bulk compositions in the Daoxian xenoliths [*Dai et al.*, 2008] do not support extensive partial melting after their formation.

[39] 4. It is possible that the heat provided by underplating melts induced significant H loss, e.g., through dehydration, in the Phanerozoic lower crust, but such thermal events did not produce any visible partial melting of the granulites (e.g., the above discussed point 3). In this case, the dehydration loss of H in the Phanerozoic granulites would be evidently larger than in the Precambrian ones. Nonetheless, the estimated difference in the extent of dehydration from their H isotopic data, mainly in the manner of H_2 loss, between the Hannuoba xenolith granulites and the Hannuoba terrain and Nushan xenolith granulites is on the first order of only about 10% (assuming they derived from mantle melts with similar δD of $-80‰$ [*Yang et al.*, 2007]), which would provide no way of accounting for the observed large difference in their water contents if their original concentrations were similar. This possibility is thus excluded.

[40] 5. Percolation of fluids dominated by CO_2 was suggested by *Newton et al.* [1980] for the formation of granulites, and such percolation would effectively remove most of the water without changing major/trace elements markedly. The effects of CO_2 on granulite-facies metamorphism have been debated, as it was argued recently that CO_2 probably plays a consequential rather than causal role in the genesis of granulites [*Cesare et al.*, 2005]. On the other hand, a pervasive percolation of CO_2 in the lower crust is in conflict with the observed intergrain $\delta^{18}O$ heterogeneity, up to 2–3‰, in intragrain homogenous samples even in <1 cm scale; such microscale variations would be erased by the fluids [*Yang*, 2008; see also *Valley and O'Neil*, 1984]. And furthermore, if granulites were really involved with CO_2 for their genesis (e.g., influx of CO_2 produces the lower water content in granulites), it would be difficult to imagine that only the Phanerozoic granulites were markedly influenced by CO_2 to lower their water contents relative to the Precambrian granulites. This possibility is therefore not favored.

[41] 6. Secondary metasomatism by melts/fluids, responsible for the formation of amphibole in the Hannuoba terrain granulites, may play some role in buffering/increasing the water content of the coexisting cpx, opx, and plag. However, it has been suggested that the formation of secondary hydrous amphibole through later alterations or metasomatism consumes nearly all of the water available in the fluid phase [*Andrut et al.*, 2003] or even in the coexisting NAMs [*Peslier et al.*, 2002]. In the former case the H content in the NAMs will remain unmodified, while in the latter case they can be notably lowered, e.g., via closed-system H redistribution. In addition, the REE patterns of mineral grains in the Hannuoba terrain samples resemble those in the Hannuoba and Nushan xenolith granulites, and no extreme variations in $(La/Yb)_N$ ratios of individual minerals can be observed between them, implying that these grains were not modified by later alteration or metasomatism [*Yang et al.*, 2007]. Finally, no hydrous phases occurring in the Nushan xenolith granulites show higher water contents.

[42] 7. For the case of water contrast being inherited from their original melts/protoliths, if the melts derived from the upper mantle, the water content of the upper mantle may have been higher in the Precambrian than in the Phanerozoic, which was then inherited by the lower crust formed from them. It is interesting to note that if the water content of the lower crust decreased from Proterozoic to Phanerozoic era, this could explain the large dispersion of water content observed for the Nushan granulites, which resided in the lower crust during this time interval. That is, the Nushan granulites may represent a mixture of Precambrian and newly formed Phanerozoic lower crust [*Huang et al.*, 2004]. In contrast, water in the Hannuoba terrain granulites could be preserved from late reequilibration because of its early exhumation.

[43] In summary, our data suggest that the Precambrian continental lower crust in eastern China was more hydrous than the Phanerozoic one and that the contrast in water contents may relate ultimately to the difference of water content in the original melts/protoliths. This may indicate that the ancient upper mantle in China was more hydrous, in agreement with the hypothesis that the upper mantle was more hydrous in the Precambrian than in the Phanerozoic [e.g., *Stone et al.*, 1997]. Several other implications from our data include the following: If the granulites formed during mantle upwelling and the source of upwelling was the deep mantle, our results would make a real difference between the upper and lower mantle degassing. Alternatively, if formation of the early lower crust was related to the occurrence of superplumes, as proposed by *Condie* [2004], and buildup of the NCC was also related to a plume, as suggested by *Zhao et al.* [2001], our results indicate that these plume-related melts were rich in water. So if superplumes accounted for the growth of the early lower crust in the NCC, the Precambrian upper mantle was not necessarily H_2O richer than the Phanerozoic upper mantle. Future research on the lower crustal granulites may shed light into which one of these hypotheses is correct.

[44] **Acknowledgments.** We thank Shun Karato, Roberta Rudnick, George Rossman, Hans Keppler, Kent Condie, John Valley, Jannick Ingrin, Elizabeth Johnson, Yigang Xu, Mingguo Zhai, and Xiaolong Huang for many helpful discussions. First review of the early version of this manuscript by Shun Karato and Yongfei Zheng helped to improve the quality; Michael Bizimis and Luigi Dallai helped to smooth the English. We thank Michael Bizimis, George Rossman, Mihai Ducea, and two anonymous reviewers for their thoughtful comments. This work was supported by the National Science Foundation of China (40673028 and 90714009), the Programme Sino-Français de Recherches Avancées (PRA T06–02), and the Hydrospec network.

References

Andrut, M., F. Brandstatter, and A. Beran (2003), Trace hydrogen zoning in diopside, *Mineral. Petrol.*, *78*, 231–241, doi:10.1007/s00710-002-0226-z.

Asimow, P. D., L. C. Stein, J. L. Mosenfelder, and G. R. Rossman (2006), Quantitative polarized infrared analysis of trace OH in populations of randomly oriented mineral grains, *Am. Mineral.*, *91*, 278–284, doi:10.2138/am.2006.1937.

Aubaud, C., E. H. Hauri, and M. M. Hirschmann (2004), Hydrogen partition coefficients between nominally anhydrous minerals and basaltic melts, *Geophys. Res. Lett.*, *31*, L20611, doi:10.1029/2004GL021341.

Bell, D. R., and G. R. Rossman (1992), Water in Earth's mantle: The role of nominally anhydrous minerals, *Science*, *255*, 1391–1397, doi:10.1126/science.255.5050.1391.

Bell, D. R., P. D. Ihinger, and G. R. Rossman (1995), Quantitative analysis of trace OH in garnet and pyroxenes, *Am. Mineral.*, *80*, 465–474.

Bell, D. R., G. R. Rossman, and R. O. Moore (2004), Abundance and partitioning of OH in a high-pressure magmatic system: Megacrysts from the Monastery kimberlite, South Africa, *J. Petrol.*, *45*, 1539–1564, doi:10.1093/petrology/egh015.

Bromiley, G. D., H. Keppler, C. McCammon, F. A. Bromiley, and S. D. Jacobsen (2004), Hydrogen solubility and speciation in natural, gem-quality chromian diopside, *Am. Mineral.*, *89*, 941–949.

Cesare, B., S. Meli, L. Nodari, and U. Russo (2005), Fe^{3+} reduction during biotite melting in graphitic metapelites: Another origin of CO_2 in granulites, *Contrib. Mineral. Petrol.*, *149*, 129–140, doi:10.1007/s00410-004-0646-3.

Chen, J. F., and B. M. Jahn (1998), Crustal evolution of southeastern China: Nd and Sr isotopic evidence, *Tectonophysics*, *284*, 101–133, doi:10.1016/S0040-1951(97)00186-8.

Chen, J., K. A. Foland, F. Xing, X. Xu, and T. Zhou (1991), Magmatism along the southeast margin of the Yangtze block: Precambrian collision of the Yangtze and Cathysia blocks of China, *Geology*, *19*, 815–818, doi:10.1130/0091-7613(1991)019<0815:MATSMO>2.3.CO;2.

Chen, S., S. Y. O'Reilly, X. Zhou, W. L. Griffin, G. Zhang, M. Sun, J. Feng, and M. Zhang (2001), Thermal and petrological structure of the lithosphere beneath Hannuoba, Sino-Korean Craton, China: Evidence from xenoliths, *Lithos*, *56*, 267–301, doi:10.1016/S0024-4937(00)00065-7.

Condie, K. C. (2004), Supercontinents and superplume event: Distinguishing signals in the geologic record, *Phys. Earth Planet. Inter.*, *146*, 319–332, doi:10.1016/j.pepi.2003.04.002.

Dai, B.-Z., S.-Y. Jiang, Y.-H. Jiang, K.-D. Zhao, and D.-Y. Liu (2008), Geochronology, geochemistry and Hf–Sr–Nd isotopic compositions of Huziyan mafic xenoliths, southern Hunan Province, south China: Petrogenesis and implications for lower crust evolution, *Lithos*, *102*, 65–87.

Deer, W. A., R. A. Howie, and J. Zussman (1992), *An Introduction to the Rock-Forming Minerals*, 2nd ed., Longman Sci. and Tech., Harlow, U. K.

Fan, Q. C., R. X. Liu, H. M. Li, N. Li, J. L. Sui, and Z. R. Lin (1998), Zircon chronology and REE geochemistry of granulite xenoliths from Hannuoba (in Chinese with English abstract), *Chin. Sci. Bull.*, *43*, 133–137.

Fan, Q. C., H. F. Zhang, J. L. Sui, M. G. Zhai, J. Sun, and N. Li (2005), Magma underplating and composition of the present crust-mantle transitional zone: Petrological and geochemical evidence from xenoliths (in Chinese with English abstract), *Sci. China, Ser. D*, *35*, 1–14.

Gao, S., W. L. Ling, Y. Qiu, Z. Lian, G. Hartmann, and K. Simon (1999), Contrasting geochemical and Sm-Nd isotopic compositions of Archean metasediments from the Kongling high-grade terrain of the Yangtze Craton: Evidence from cratonic evolution and redistribution of REE during crustal anatexis—Evidence for a 3.0-Ga con, *Geochim. Cosmochim. Acta*, *63*, 2071–2088.

Grant, K., J. Ingrin, J. P. Lorand, and P. Dumas (2007), Water partitioning between mantle minerals from peridotite xenoliths, *Contrib. Mineral. Petrol.*, *154*, 15–34, doi:10.1007/s00410-006-0177-1.

Griffin, W. L., A. D. Zhang, S. Y. O'Reilly, and C. G. Ryan (1998), Phanerozoic evolution of the lithosphere beneath the Sino-Korean Craton, in *Mantle Dynamics and Plate Interactions in East Asia*, *Geodyn. Ser.*, vol. 27, edited by M. F. J. Flower et al., pp. 107–126, AGU, Washington, D. C.

Guo, F., Y. L. Wu, W. M. Fan, and G. Lin (1996), A petrological study of the gabbro xenoliths from Mesozoic basalts in Ningyuan-Daoxian, Hunan (in Chinese with English abstract), *Geotecton. Metallog.*, *20*, 38–45.

Guo, J. H., M. Sun, F. K. Chen, and M. G. Zhai (2005), Sm–Nd and SHRIMP U–Pb zircon geochronology of high-pressure granulites in the Sanggan area, North China Craton: Timing of Paleoproterozoic continental collision, *J. Asian Earth Sci.*, *24*, 629–642, doi:10.1016/j.jseaes.2004.01.017.

Hauri, E. H., G. A. Gaetani, and T. H. Green (2006), Partitioning of water during melting of the Earth's upper mantle at H_2O-undersaturated conditions, *Earth Planet. Sci. Lett.*, *248*, 715–734, doi:10.1016/j.epsl.2006.06.014.

Huang, X.-L., Y.-G. Xu, and D.-Y. Liu (2004), Geochronology, petrology and geochemistry of the granulite xenoliths from Nushan, east China: Implication for a heterogeneous lower crust beneath the Sino-Korean Craton, *Geochim. Cosmochim. Acta*, *68*, 127–149, doi:10.1016/S0016-7037(03)00416-2.

Ingrin, J., and H. Skogby (2000), Hydrogen in nominally anhydrous upper-mantle minerals: Concentration levels and implications, *Eur. J. Mineral.*, *12*, 543–570.

Johnson, E. A. (2006), Water in nominally anhydrous crustal minerals: Speciation, concentration, and geologic significance, in *Water in Nominally Anhydrous Minerals*, edited by H. Keppler and J. R. Smyth, pp. 117–154, Mineral. Soc. of Am., Washington, D. C.

Johnson, E. A., and G. R. Rossman (2003), The concentration and speciation of hydrogen in feldspars using FTIR and H-1 MAS NMR spectroscopy, *Am. Mineral.*, *88*, 901–911.

Johnson, E. A., and G. R. Rossman (2004), A survey of hydrous species and concentrations in igneous feldspars, *Am. Mineral.*, *89*, 586–600.

Katayama, I., and S. Nakashima (2003), Hydroxyl in clinopyroxene from the deep subducted crust: Evidence for H_2O transport into mantle, *Am. Mineral.*, *88*, 229–234.

Katayama, I., S. Nakashima, and H. Yurimoto (2006), Water content in natural eclogite and implication for water transport into the deep upper mantle, *Lithos*, *86*, 245–259, doi:10.1016/j.lithos.2005.06.006.

Keppler, H., and J. R. Smyth (2006), *Water in Nominally Anhydrous Minerals*, 478 pp., Mineral. Soc. of Am., Washington, D. C.

Koga, K., E. Hauri, M. Hirschmann, and D. Bell (2003), Hydrogen concentration analyses using SIMS and FTIR: Comparison and calibration for nominally anhydrous minerals, *Geochem. Geophys. Geosyst.*, *4*(2), 1019, doi:10.1029/2002GC000378.

Kovács, I., J. Hermann, H. S. C. O'Neill, J. Fitz Gerald, M. Sambridge, and G. Horváth (2008), Quantitative absorbance spectroscopy with unpolarized light: Part II. Experimental evaluation and development of a protocol for quantitative analysis of mineral IR spectra, *Am. Mineral.*, *93*, 765–778, doi:10.2138/am.2008.2656.

Langer, K., E. Robarick, N. V. Sobolev, V. S. Shatsky, and W. Wang (1993), Single-crystal spectra of garnets from diamondiferous high-pressure metamorphic rocks from Kazakhstan: Indications for OH^-, H_2O, and FeTi charge transfer, *Eur. J. Mineral.*, *5*, 1091–1100.

Li, X.-H., S.-L. Chung, H. Zhou, C.-H. Lo, Y. Liu, and C.-H. Chen (2004), Jurassic intraplate magmatism in southern Hunan-eastern Guangxi: $^{40}Ar/^{39}Ar$ dating, geochemistry, Sr-Nd isotopes and implications for the tectonic evolution of SE China, *Geol. Soc. Spec. Publ.*, *226*, 193–215.

Li, Z.-X., and X.-H. Li (2007), Formation of the 1300-km-wide intracontinental orogen and postorogenic magmatic province in Mesozoic south China: A flat-slab subduction model, *Geology*, *35*, 179–182, doi:10.1130/G23193A.1.

Li, Z.-X., X. Li, H. Zhou, and P. D. Kinny (2002), Grenvillian continental collision in south China: New SHRIMP U-Pb zircon results and implications for the configuration of Rodinia, *Geology*, *30*, 163–166, doi:10.1130/0091-7613(2002)030<0163:GCCISC>2.0.CO;2.

Libowitzky, E., and G. R. Rossman (1996), Principles of quantitative absorbance measurements in anisotropic crystals, *Phys. Chem. Miner.*, *23*, 319–327, doi:10.1007/BF00199497.

Liu, D. Y., A. P. Nutman, W. Compston, J. S. Wu, and Q. H. Shen (1992), Remnants of ≥3800 Ma crust in the Chinese part of the Sino-Korean Craton, *Geology*, *20*, 339–342, doi:10.1130/0091-7613(1992)020<0339:ROMCIT>2.3.CO;2.

Liu, Y.-S., S. Gao, S.-Y. Jin, S.-H. Hu, M. Sun, Z.-B. Zhao, and J.-L. Feng (2001), Geochemistry of lower crustal xenoliths from Neogene Hannuoba basalt, North China Craton: Implications for petrogenesis and lower crustal composition, *Geochim. Cosmochim. Acta*, *65*, 2589–2604, doi:10.1016/S0016-7037(01)00609-3.

Menzies, M. A., W. M. Fan, and M. Zhang (1993), Palaeozoic and Cenozoic lithoprobes and loss of >120 km of Archean lithosphere, Sino-Korean Craton, in *Magmatic Processes and Plate Tectonics*, edited by H. M. Prichard et al., *Geol. Soc. Spec. Publ.*, *76*, 71–81.

Mierdel, K., H. Keppler, J. R. Smyth, and F. Langenhorst (2007), Water solubility in aluminous orthopyroxene and the origin of Earth's asthenosphere, *Science*, *315*, 364–368, doi:10.1126/science.1135422.

Newton, R. C., J. V. Smith, and B. F. Windley (1980), Carbonic metamorphism, granulites and crustal growth, *Nature*, *288*, 45–50, doi:10.1038/288045a0.

Paterson, M. S. (1982), The determination of hydroxyl by infrared absorption in quartz, silicate glasses and similar materials, *Bull. Mineral.*, *105*, 20–29.

Peslier, A. H., and J. F. Luhr (2006), Hydrogen loss from olivines in mantle xenoliths from Simcoe (USA) and Mexico: Mafic alkalic magma ascent rates and water budget of the sub-continental lithosphere, *Earth Planet. Sci. Lett.*, *242*, 302–319, doi:10.1016/j.epsl.2005.12.019.

Peslier, A. H., J. F. Luhr, and J. Post (2002), Low water contents in pyroxenes from spinel-peridotites of the oxidized, sub-arc mantle wedge, *Earth Planet. Sci. Lett.*, *201*, 69–86, doi:10.1016/S0012-821X(02)00663-5.

Pouchou, J. L., and F. Pichoir (1985), 'PAP' (φ-ρ-Z) correction procedure for improved quantitative microanalysis, in *Microbeam Analysis*, edited by J. T. Armstrong, pp. 104–106, San Francisco Press, San Francisco, Calif.

Qiu, Y. M., S. Gao, N. J. McNaughton, D. I. Groves, and W. Ling (2000), First evidence of >3.2 Ga continental crust in the Yangtze Craton of south China and its implications for Archean crustal evolution and Phanerozoic

tectonics, *Geology*, *28*, 11–14, doi:10.1130/0091-7613(2000)028<0011:FEOGCC>2.0.CO;2.
Rauch, M., and H. Keppler (2002), Water solubility in orthopyroxene, *Contrib. Mineral. Petrol.*, *143*, 525–536.
Rossman, G. R., and R. D. Aines (1991), The hydrous components in garnets: Grossular-hydrogrossular, *Am. Mineral.*, *76*, 1153–1164.
Rossman, G. R., A. Beran, and K. Langer (1989), The hydrous component of pyrope from the Dora Maira Massif, Western Alps, *Eur. J. Mineral.*, *1*, 151–154.
Rudnick, R. L. (1992), Xenoliths—Samples of the lower continental crust, in *Continental Lower Crust*, edited by D. M. Fountain et al., pp. 269–316, Elsevier, Amsterdam.
Rudnick, R. L., and D. M. Fountain (1995), Nature and composition of the continental crust: A lower crustal perspective, *Rev. Geophys.*, *33*, 267–309, doi:10.1029/95RG01302.
Sambridge, M., J. Fitz Gerald, I. Kovács, H. S. C. O'Neill, and J. Hermann (2008), Quantitative absorbance spectroscopy with unpolarized light: Part I. Physical and mathematical development, *Am. Mineral.*, *93*, 751–764, doi:10.2138/am.2008.2657.
Shu, L., and J. Charvet (1996), Kinematics and geochronology of the Proterozoic Dongxiang-Shexian ductile shear zone: With HP metamorphism and ophiolitic melange (Jiangnan region, south China), *Tectonophysics*, *267*, 291–302, doi:10.1016/S0040-1951(96)00104-7.
Skogby, H., and G. R. Rossman (1989), OH^- in pyroxene: An experimental study of incorporation mechanisms and stability, *Am. Mineral.*, *74*, 1059–1069.
Skogby, H., D. R. Bell, and G. R. Rossman (1990), Hydroxide in pyroxene; variations in the natural environment, *Am. Mineral.*, *75*, 764–774.
Stalder, R. (2004), Influence of Fe, Cr and Al on hydrogen incorporation in orthopyroxene, *Eur. J. Mineral.*, *16*, 703–711, doi:10.1127/0935-1221/2004/0016-0703.
Stalder, R., and H. Skogby (2002), Hydrogen incorporation in enstatite, *Eur. J. Mineral.*, *14*, 1139–1144, doi:10.1127/0935-1221/2002/0014-1139.
Stone, W. E., E. Deloule, M. S. Larson, and C. M. Lesher (1997), Evidence for hydrous high-MgO melts in the Precambrian, *Geology*, *25*, 143–146, doi:10.1130/0091-7613(1997)025<0143:EFHHMM>2.3.CO;2.
Toramaru, A., and N. Fujii (1986), Connectivity of melt phase in a partially molten peridotite, *J. Geophys. Res.*, *91*, 9239–9252, doi:10.1029/JB091iB09p09239.
Valley, J. W., and J. R. O'Neil (1984), Fluid heterogeneity during granulite facies metamorphism in the Adirondacks: Stable isotope evidence, *Contrib. Mineral. Petrol.*, *85*, 158–173, doi:10.1007/BF00371706.
Waff, H. S., and J. R. Bulau (1979), Equilibrium fluid distribution in an ultramafic partial melt under hydrostatic stress conditions, *J. Geophys. Res.*, *84*, 6109–6114, doi:10.1029/JB084iB11p06109.
Wells, P. R. A. (1977), Pyroxene thermometry in simple and complex systems, *Contrib. Mineral. Petrol.*, *62*, 129–139, doi:10.1007/BF00372872.
Wilde, S. A., X. Zhou, A. A. Nemchin, and M. Sun (2003), Mesozoic crust-mantle interaction beneath the North China Craton: A consequence of the dispersal of Gondwanaland and accretion of Asia, *Geology*, *31*, 817–820, doi:10.1130/G19489.1.
Wood, B. J. (1974), The solubility of alumina in orthopyroxene coexisting with garnet, *Contrib. Mineral. Petrol.*, *46*, 1–15, doi:10.1007/BF00377989.
Wood, B. J., and S. Banno (1973), Garnet-othopyroxene and orthopyroxene-clinopyroxene relationships in simple and complex systems, *Contrib. Mineral. Petrol.*, *42*, 109–124, doi:10.1007/BF00371501.
Xia, Q.-K., Y.-M. Sheng, X.-Z. Yang, and H.-M. Yu (2005), Heterogeneity of water in garnets from UHP eclogites, eastern Dabieshan, China, *Chem. Geol.*, *224*, 237–246, doi:10.1016/j.chemgeo.2005.08.003.
Xia, Q.-K., X.-Z. Yang, E. Deloule, Y.-M. Sheng, and Y.-T. Hao (2006), Water in the lower crustal granulite xenoliths from Nushan, eastern China, *J. Geophys. Res.*, *111*, B11202, doi:10.1029/2006JB004296.
Xu, X., S. Y. O'Reilly, W. L. Griffin, X. Zhou, and X. Huang (1998), The nature of the Cenozoic lithosphere at Nushan, eastern China, in *Mantle Dynamics and Plate Interaction in East Asia*, *Geodyn. Ser.*, vol. 27, edited by M. F. J. Flower et al., pp. 167–196, AGU, Washington, D. C.
Yang, X. Z. (2008), Water content and H-O-Li isotopes in lower crustal granulite minerals of eastern China, Ph.D. thesis, 247 pp., Univ. of Sci. and Technol. of China, Hefei, China.
Yang, X. Z., E. Deloule, and Q. K. Xia (2007), Tracing water exchange between mantle and continental crust with δD values of NAMs in granulite, paper presented at Goldschmidt Conference, Geochem. Soc., Cologne, Germany.
Zhai, M.-G., J.-H. Guo, and W.-J. Liu (2001), An exposed cross-section of early Precambrian continental lower crust in North China Craton, *Phys. Chem. Earth, Part A*, *26*, 781–792, doi:10.1016/S1464-1895(01)00127-2.
Zhai, M., J. Guo, and W. Liu (2005), Neoarchean to Paleoproterozoic continental evolution and tectonic history of the North China Craton: A review, *J. Asian Earth Sci.*, *24*, 547–561, doi:10.1016/j.jseaes.2004.01.018.
Zhang, S.-B., Y.-F. Yong, Y.-B. Wu, Z.-F. Zhao, S. Gao, and F.-Y. Wu (2006), Zircon isotope evidence for $\geq$3.5 Ga continental crust in the Yangtze Craton of China, *Precambrian Res.*, *146*, 16–34, doi:10.1016/j.precamres.2006.01.002.
Zhao, G., S. A. Wilde, P. A. Cawood, and M. Sun (2001), Archean blocks and their boundaries in the North China Craton: Lithological, geochemical, structural and P–T path constraints and tectonic evolution, *Precambrian Res.*, *107*, 45–73, doi:10.1016/S0301-9268(00)00154-6.
Zhao, Z. H., Z. W. Bao, and B. Y. Zhang (1998), Geochemistry of the Mesozoic basaltic rocks in southern Hunan Province (in Chinese with English abstract), *Sci. China, Ser. D*, *41*, 102–112.
Zheng, J., W. L. Griffin, S. Y. O'Reilly, M. Zhang, N. Pearson, and Y. Pan (2006), Widespread Archean basement beneath the Yangtze Craton, *Geology*, *34*, 417–420, doi:10.1130/G22282.1.

E. Deloule, Centre de Recherches Pétrographiques et Géochimiques, Centre National de la Recherches Scientifique, BP 20, Vandoeuvre-les-Nancy CEDEX, F-54501 France.

Q.-C. Fan, Institute of Geology, China Earthquake Administration, Beijing 10029, China.

M. Feng, Q.-K. Xia, and X.-Z. Yang (corresponding author), CAS Key Laboratory of Crust-Mantle Materials and Environments, School of Earth and Space Sciences, University of Science and Technology of China, Hefei 230026, China. (qkxia@ustc.edu.cn)